Antarctic Science 29(5), 429–444 (2017) © Antarctic Science Ltd 2017 doi:10.1017/S0954102017000116

Sedimentary analysis and magnetic properties of Lake Anónima, Vega Island

MARCOS A.E. CHAPARRO[1], MAURO A.E. CHAPARRO[2], FRANCISCO E. CÓRDOBA[3], KARINA L. LECOMTE[4,5], JOSÉ D. GARGIULO[1], ANA M. BARRIOS[6], GIMENA M. URÁN[5], NADIA T. MANOGRASSO CZALBOWSKI[7], ARACELI LAVAT[8] and HARALD N. BÖHNEL[9]

[1]*Centro de Investigaciones en Física e Ingeniería del Centro de la Provincia de Buenos Aires (CIFICEN, CONICET-UNCPBA), Pinto 399, 7000 Tandil, Argentina*
[2]*Centro Marplatense de Investigaciones Matemáticas (CEMIM), Facultad de Ciencias Exactas y Naturales UNMDP, CONICET, Mar del Plata, Argentina*
[3]*Instituto de Ecorregiones Andinas (INECOA), Universidad Nacional de Jujuy-CONICET. Instituto de Geología y Minería, Av. Bolivia 1661 (4600), San Salvador de Jujuy, Argentina*
[4]*Centro de Investigaciones en Ciencias de la Tierra (CICTERRA), CONICET Av. Vélez Sarsfield 1611, X5016GCA Córdoba, Argentina*
[5]*Universidad Nacional de Córdoba, Facultad de Ciencias Exactas Físicas y Naturales, Av. Vélez Sarsfield 1611, X5016CGA Córdoba, Argentina*
[6]*Universidad de Granada, Av. del Hospicio, s/n, 18010 Granada, Spain*
[7]*Instituto Antártico Argentino (IAA), 25 De Mayo 1143, San Martín, Provincia de Buenos Aires, Argentina*
[8]*Centro de Investigaciones en Física e Ingeniería del Centro de la Provincia de Buenos Aires (CIFICEN, CONICET-UNCPBA), Olavarría, Argentina*
[9]*Centro de Geociencias (UNAM), Blvd. Juriquilla 3001, 76230 Querétaro, México*
chapator@exa.unicen.edu.ar

Abstract: During the summer Lake Anónima experiences important changes in salinity and lake level fluctuations. Physicochemical data and field observations indicate that evaporative processes are dominant and that the water inflow is mainly provided by snow meltwater and streams. A multiproxy analysis of data from lake bottom sediments suggests that the main surface stream located south-west of the lake controls the clastic input and the spatial variation of sediment composition. Through an integrated analysis (magnetic, X-ray diffraction and Fourier transform infrared spectroscopy studies) magnetite and greigite minerals were identified in these lake sediments. Such ferrimagnetic minerals have ultra-fine grain sizes (< 0.1 μm). Magnetic parameters and non-magnetic variables analysed by multivariate statistics reveal significant differences between silt facies (e.g. mass-specific susceptibility $\chi = 109.6 \times 10^{-8}\,m^3\,kg^{-1}$, remanent coercivity $H_{cr} = 49.2$ mT and total organic carbon (TOC) = 1.11%) and sand facies (e.g. $\chi = 82.1 \times 10^{-8}\,m^3\,kg^{-1}$, $H_{cr} = 44.7$ mT and TOC = 0.70%), and four recent depositional sub-environments were identified and characterized in Lake Anónima. This multiparameter analysis contributes to the understanding of present-day lacustrine dynamic and sedimentary processes. Lake Anónima may provide a useful analogue for the interpretation of other lacustrine basins in the Antarctic region.

Received 17 October 2016, accepted 2 February 2017, first published online 4 May 2017

Key words: Antarctica, environmental magnetism, grain size analysis, hydrochemical studies, lake sediments, multivariate statistics

Introduction

Antarctica as a remote and mostly unpopulated region provides a unique opportunity for studying recent environmental changes associated with the current climate change (King *et al.* 2004, Hodgson *et al.* 2013, Lecomte *et al.* 2016), as well as those related to adverse anthropogenic impacts of Antarctic stations (e.g. Chaparro *et al.* 2007). Knowledge of different processes impacting on Antarctica is fundamental for understanding the effects of future environmental and climate changes in this polar region (Lecomte *et al.* 2016).

Antarctic lakes and ponds are especially sensitive to changes in the hydrological balance, which are, in turn, the result of climatic fluctuations (e.g. Björck *et al.* 1996, Hodgson *et al.* 2013, Hawes *et al.* 2014). These fluctuations in the hydrological balance are reflected by variations in lake levels, sediment input, chemistry and biology of the water column, and the sedimentary processes, which are recorded in the sediments (Warrier *et al.* 2014). Lacustrine sediments carry a strong signal originating from minerogenic and chemical weathering products of the catchment areas (i.e. solutes and particulate material) and can be

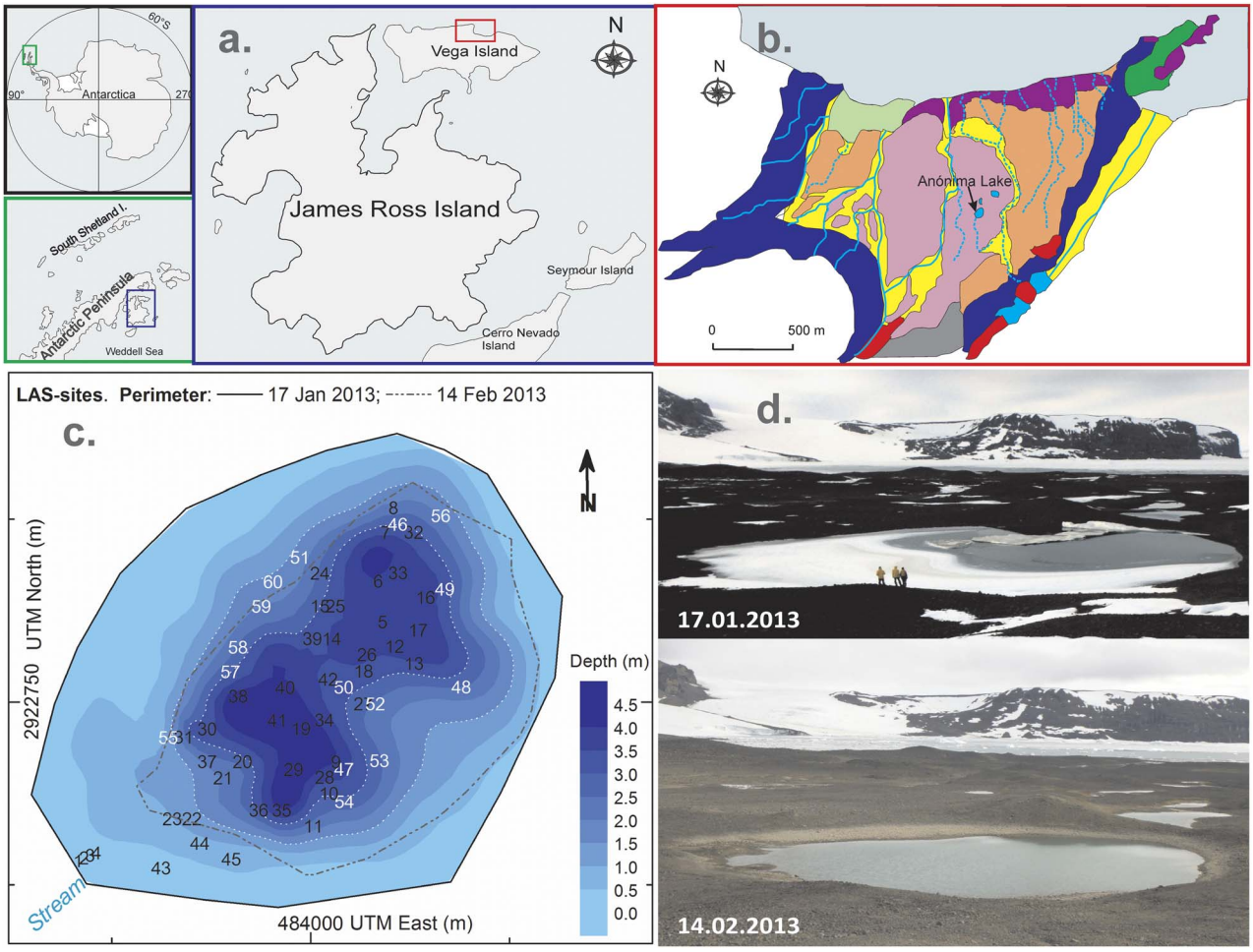

Fig. 1a. Map of the Antarctic continent, Antarctic Peninsula and James Ross Archipelago. **b.** Lake Anónima location and surrounding geology (modified from Ermolin *et al.* 2002). Glacial and snow meltwater creeks and lakes are shown in cyan and glaciers are in white. Present sediments: glaciofluvial (yellow), deltaic (light green) and marine (green), Holocene sediments: glaciofluvial (orange), marine/deltaic (purple) and Till (light purple), Tertiary outcrops James Ross Volcanic Group (red). **c.** Lake bathymetry (during summer) and shore lines in January and February. Sampling localities are shown by sample number, with a total of 45 sediment samples (from 60 sites) collected from the top of the sediment column. Sites (without sediment) with basaltic blocks and gravel are indicated by a number in white. **d.** The system shows significant hydrological change during the summer (photographs taken in January and February 2013).

considered to be representatives of sedimentological and biogeochemical processes taking place in the watershed (Alfonso *et al.* 2015).

A wide variety of studies have conducted magnetic measurements in order to investigate environmental and anthropogenic processes in lake systems (e.g. Pan *et al.* 2005, Chaparro *et al.* 2014). Iron oxides are very sensitive to physicochemical conditions in sedimentary environments and their magnetic properties can be determined using environmental magnetism methods (Liu *et al.* 2012). Magnetic properties are well suited as proxies of magnetic mineral concentration, magnetic grain size and environmental processes affecting these parameters (Maher *et al.* 1999, Egli 2004). Magnetic properties are controlled by the competing fluxes of allochthonous and autochthonous magnetic particles, and differ according to location in a lake basin (Lascu *et al.* 2012). So far, studies of the magnetic properties of Antarctic lacustrine sediments are limited (Chaparro *et al.* 2014, Warrier *et al.* 2014, Lecomte *et al.* 2016). Knowledge of the spatial distribution and limnologic control of magnetic properties and non-magnetic sedimentological parameters in Antarctic lakes is required to improve our understanding of environmental processes, as well as for development of better palaeoenvironmental and palaeoclimate reconstructions (Lascu & Plank 2013).

In this study, the distribution of detailed magnetic properties and additional non-magnetic data (grain size and total organic carbon (TOC)) of sediments from across

https://doi.org/10.1017/S0954102017000116 Published online by Cambridge University Press

Lake Anónima (LA) was investigated to unravel the sedimentary and geochemical processes in the lake and its surroundings. The main aim of the analysis was focused on determining magnetic proxies of surface sediments for understanding environmental dynamics, i.e. recent depositional processes.

Geological setting

Lake Anónima is located at Bahía del Diablo on Vega Island (James Ross Archipelago, Antarctic Peninsula; Fig. 1a). It is part of an endorheic basin situated in a glacial valley developed on Late Cretaceous sedimentary rocks and Tertiary volcanic rocks. The first lithologic group consists of a set of fossiliferous marine shales and sandstones of Santa Marta, Snow Hill Island and López de Bertodano formations (Roberts *et al.* 2014), and the second is basalt of the James Ross Island Volcanic Group (Fig. 1b). The bottom of the valley is filled mainly with Holocene till deposits of local basaltic and, in a lower proportion, sediment clasts (Zale & Karlen 1989, Ermolin *et al.* 2002). Along the northern coast of Bahía del Diablo, deltaic and marine deposits produced by marine ingressions after the early Holocene deglaciation are interbedded with till deposits. In the southern part of the valley, moraine deposits were partially reworked and are covered by Holocene and recent glaciofluvial sediment (Ermolin *et al.* 2002).

Lake Anónima is a shallow basal-moraine lake, which originated by thermokarst. It is a proglacial lake with water input from streams and snow meltwater with a sediment load that has formed a small delta on the south-west coast of the lake. The lake has a maximum depth of 4.6 m and there are two deep sub-basins separated by a shallow ridge (Fig. 1c).

The climate in the James Ross Archipelago is semi-arid with annual snowfall ranging from 200–500 mm yr^{-1} w.e. (water equivalent of precipitation; Strelin & Sone 1998). Summers are short (December–February) and mean temperatures for the warmest and coldest months at Marambio Station (64°14'S, 56°38'W) are -3.3°C and -14.5°C, respectively (data available from the National Meteorological Service Argentina, Marambio Station). During winter the lake surface is frozen and snow accumulates on the surface. With increasing temperatures in late spring and early summer, first the snow starts to melt, followed by thawing of the ice layer. When the mean temperature is high enough, the permafrost develops an active layer, putting the complete water cycle into operation. Lake Anónima collects surface runoff and can drain underground into surface streams and nearby lake systems. Terrestrial vegetation on Vega Island is limited to non-vascular plants, predominantly bryophytes and lichen tundra.

Methods

Sampling

Stream, snow and lake bottom sediment samples were taken from the system during the summer Antarctic campaign in 2012–13 (CAV-2012/2013 Dirección Nacional del Antártico, Argentina).

The bottom sediment samples were collected using an inflatable boat at 45 of 60 points distributed in a grid covering all present-day depositional environments (Fig. 1c). An Ekman dredger was slowly lowered to capture the uppermost sediments. The top 2–3 cm were skimmed, and refrigerated until their analysis. Co-ordinates of each sampling site were recorded using a GPS receiver, and water depth was recorded either using sonar or manually for shallow littoral areas. In the laboratory, each sediment sample was prepared and sub-sampled for magnetic, grain size and geochemical analyses.

Snow and stream samples were collected following standardized techniques (e.g. Namiesnik & Szefer 2010), to compare geochemical signatures of different sources: atmospheric and tributaries. Lakewater was sampled twice, on 17 January and 12 February 2013, to evaluate the physicochemical changes. Water temperature, pH, electrical conductivity, total dissolved solids (TDS) and alkalinity were measured *in situ*. Alkalinity was measured as $CaCO_3$, using a 0.16 N H_2SO_4 solution until pH = 4.5. Endpoint titration was reached in unfiltered water. For subsequent determinations, samples were vacuum filtered in the field with 0.22 µm pore-size cellulose filters (HA-type, Millipore). One aliquot was stored in polyethylene bottles at 4°C for the determination of anions by chemically suppressed ion chromatography with conductivity detection. Another aliquot was acidified ($pH < 2$) with concentrated, redistilled and ultrapure HNO_3 (Sigma-Aldrich) for the analytical determination of major, minor and trace elements by inductively coupled plasma-mass spectrometry (ICP-MS, Activation Laboratories, Ancaster, ON, Canada). The results for major, minor and trace elements were validated using NIST (National Institute of Standards and Technology) 1640 and Riverine Water Reference Materials for Trace Metals certified by the National Research Council of Canada (SRLS-4).

Grain size and geochemical studies

Grain sizes were determined by laser diffraction with a Horiba LA-950 particle size analyser at the Centro de Investigaciones en Ciencias de la Tierra (Universidad Nacional de Cordoba, Argentina). Sediments were pre-treated with Na_2PO_7 (2% w/v, 24 h) for deflocculating

https://doi.org/10.1017/S0954102017000116 Published online by Cambridge University Press

Table I. Physicochemical characteristics of Lake Anónima.

	Sample name				
	2N-BD-1	2N-BD-2	2R-LA-1	2L-LA-1	2L-LA-2
Date	23 Jan 2013	15 Feb 2013	26 Jan 2013	17 Jan 2013	12 Feb 2013
Type of sample	Snow	Snow	Spring	Lake	Lake
pH	6.48	5.48	8.24	7.37	8.14
Conductivity, µS cm^{-1}	18.4	27.3	214	134.7	154.1
TDS, mg l^{-1}	9.2	13.7	108.1	67.3	77
HCO_3^-	610	620	42 090	18 178	61 020
Cl^-	1380	1065	63 610	33 120	13 820
SO_4^{2-}	780	450	15 800	7710	2520
Mg	96	210	4280	2710	3340
Ca	500	300	11 900	5700	7100
Na	436	709	24 400	16 600	18 700
K	110	340	1480	1400	1260
Si	< 200	< 200	5300	3000	3400
Al	59	143	57	21	147
Ti	4.2	9.3	5.7	1	11
V	0.2	0.3	4.6	2.1	3.2
Fe	40	170	120	10	160
Co	0.037	0.137	0.118	0.029	0.139
Cu	0.6	2.4	1.7	0.9	1.8
Rb	0.136	0.325	0.433	0.235	0.554
Sr	0.92	1.88	10.4	7.31	7.95
Ba	0.6	0.6	1.1	0.3	1.7
U	0.003	0.006	0.045	0.015	0.026
∑REE	0.132	0.468	0.232	0.078	0.339

REE = rare earth element, TDS = total dissolved solids.
Elements are given in µg l^{-1}.

clay, and then rinsed four times with distilled water. Thereafter, they were treated with 35% HCl for 24 h to remove carbonates, and washed four times with distilled water. Finally, after adding 10 ml of 30% H_2O_2 to eliminate organic matter (OM), the samples were boiled for 4 h and rinsed five times with distilled water. Samples were minimally dispersed to prevent the breaking up of aggregates. The precision (reproducibility) of the laser diffraction particle sizer was tested using mixtures of glass beads (NIST traceable polydisperse particle standard PS202/3–30 µm and PS215/10–100 µm; Whitehouse Scientific). For both runs (PS202, $n = 6$ and PS215, $n = 5$) the median (D50) was within 3% certified nominal value, and the percentiles D10 and D90 were within 5% of nominal values for the standards. This instrument yields the following grain size classes: coarse–medium sand D (> 250 µm), fine sand C (125–250 µm), very fine sand B (63–125 µm), coarse silt A5 (31.2–63 µm), medium silt A4 (15.6–31.2 µm), fine silt A3 (7.8–15.6 µm), very fine silt A2 (3.9–7.8 µm) and clay A1 (< 3.9 µm).

Total inorganic carbon (TIC) and TOC content in all samples was estimated by loss on ignition (LOI; Heiri *et al.* 2001). All LOI analyses were carried out in a muffle furnace. The samples were heated at 105°C for 24 h, then at 550°C for 4 h and at 950°C for 2 h. After each step, the dry weight (DW) of the sample was obtained. The following equations were used to calculate the percentage of LOI at 550°C and 950°C:

$$LOI_{550} = 100(DW_{105} - DW_{550}) / WS, \quad (1)$$

$$LOI_{950} = 100(DW_{550} - DW_{950}) / WS, \quad (2)$$

where WS is the initial weight of the sample and DW_{105}, DW_{550} and DW_{950} are the dry weight of the sample after heating at 105°C, 550°C and 950°C, respectively.

The remaining sample, after heating, is the residuum (LOI_{res}) associated with siliciclastic material. LOI_{550} and LOI_{950} were used to determine TOC and TIC content by Dean's relations (TOC = LOI_{550}/2, TIC = 0.273 LOI_{950}) (Dean 1974, 1999).

Magnetic studies

Magnetic proxies can be determined with high sensitivity combined with fast laboratory processing. Sample preparation is relatively simple, laboratory instruments are of relatively low cost, and most measurements are non-destructive. Magnetic measurements were carried out in the Laboratory of Paleomagnetism and Rock-magnetism at Centro de Investigaciones en Física e Ingeniería del Centro de la Provincia de Buenos Aires (Universidad Nacional del Centro de la Provincia de Buenos Aires,

https://doi.org/10.1017/S0954102017000116 Published online by Cambridge University Press

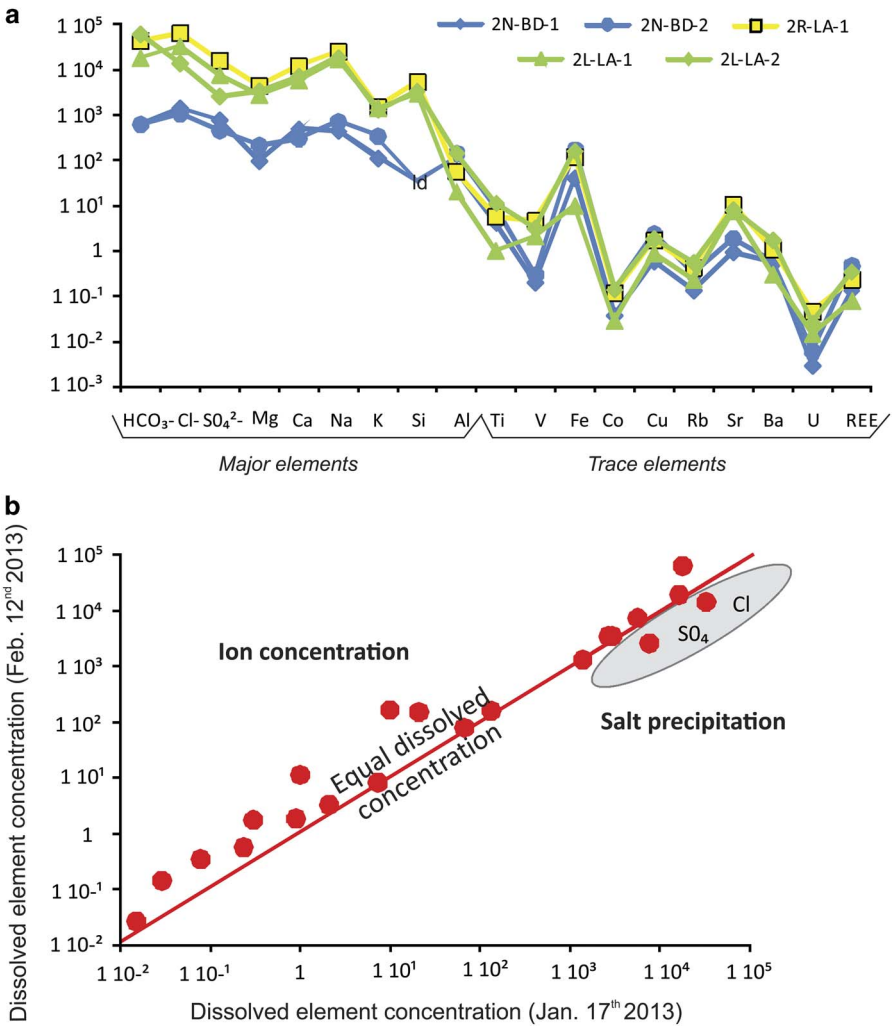

Fig. 2a. Dissolved major and trace element concentrations from snow (2N-BD-1 and 2), stream water (2R-LA-1) and lake water (2L-LA-1 and 2). **b.** Geochemical data show an increase in dissolved element concentration in a short period of ~1 month.

Argentina) and at the Centro de Geociencias (Universidad Nacional Autónoma de México).

A small amount of material (< 50 mg) was used to measure with a Princeton Measurement Micromag 2900 AGM system magnetic hysteresis loops and isothermal remanent magnetizations in fields between -2 and 2 T and at room temperature. The material was weighed to allow for calculation of mass-corrected hysteresis parameters. Among hysteresis parameters and ratios of interest, the saturation magnetization (M_s), saturation remanence (M_r), coercive force (H_c) and the relative contribution of paramagnetic and diamagnetic minerals to the M_s were calculated.

Sediment samples were also sub-sampled and packed into plastic containers (2.3 cm^3), weighed (2–3 g) and their magnetic susceptibility, anhysteretic (ARM) and isothermal remanent magnetization (IRM) measured. Volumetric magnetic susceptibility (κ) was measured with a Bartington Instruments MS2 and a MS2B dual frequency sensor (0.47 and 4.7 kHz). χ was obtained by taking into account the sample mass. The ARM was imparted using an alternating field (AF) demagnetizer by superimposing a direct current (DC) bias field of 50 μT in the AF interval 100–2.5 mT, and the ARM was measured with a Minispin magnetometer (Molspin). The mass-specific ARM susceptibility (χ_{ARM}) was estimated from the ARM acquired in this DC bias field. The χ_{ARM}/χ-ratio and the King's plot (χ_{ARM} *vs* χ, King *et al.* 1982) were also studied. The IRM acquisition curves and the saturation of IRM (SIRM = $IRM_{2.5T}$) were determined in 25 steps between 10 mT and 2.5 T. The IRM was produced with an ASC Scientific pulse magnetizer, and measured with the Minispin magnetometer. H_{cr}, S-ratio (= $-IRM_{-300mT}$/SIRM), χ_{ARM}/SIRM and SIRM/χ ratio were also calculated.

Some samples (of ~100–220 mg) were studied in a laboratory-built horizontal magnetic balance to produce thermomagnetic curves. The induced field was chosen at

https://doi.org/10.1017/S0954102017000116 Published online by Cambridge University Press

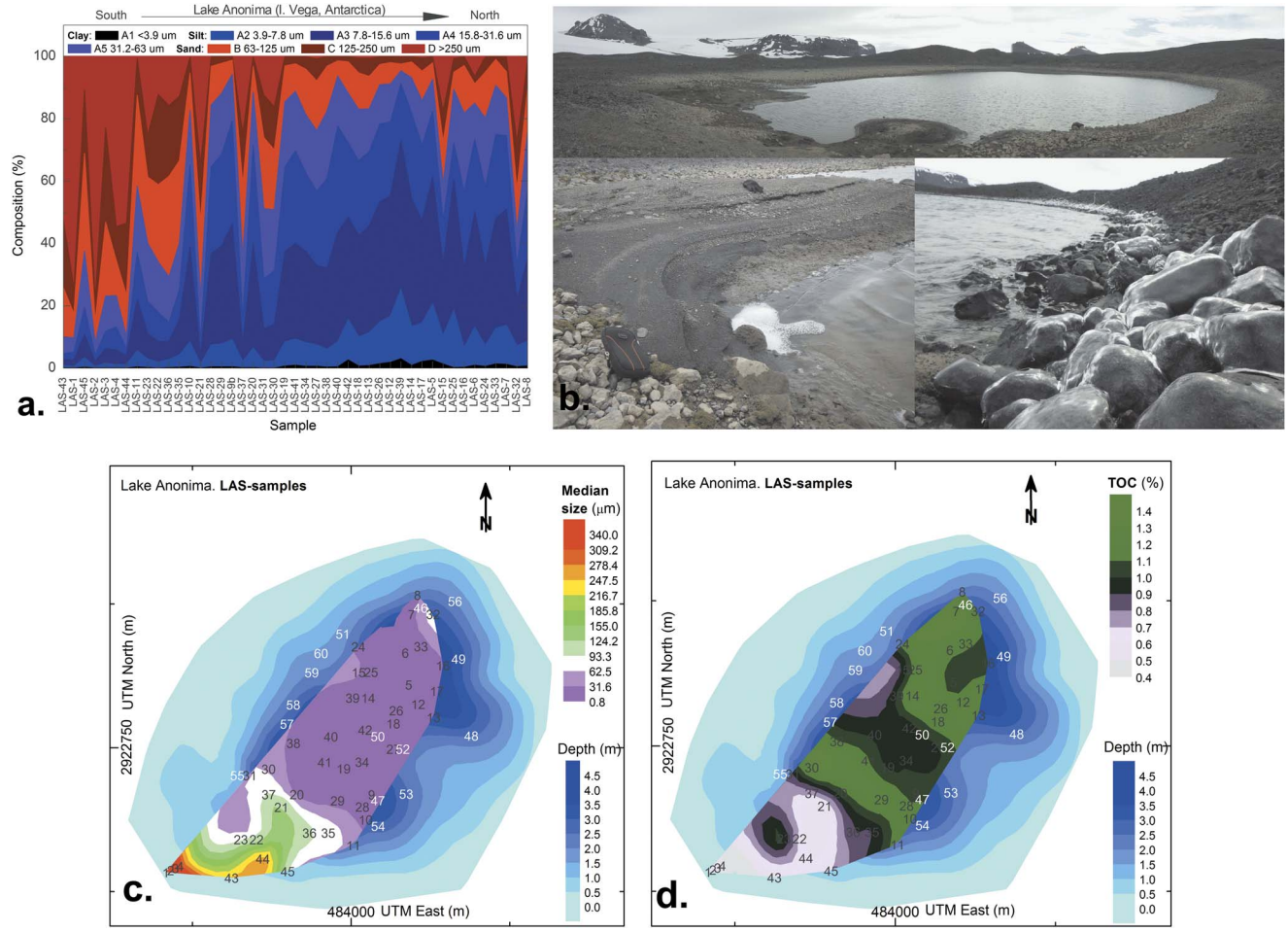

Fig. 3a. Percentage contribution of sand, silt and clay grain size fractions, in order of sample locations from south to north. **b.** Panoramic view of Lake Anónima. View of the deltaic area developed by the surface main stream inflow on the south-west margin of the lake (upper image) and details of sand, basaltic blocks and gravel at the littoral margin of the lake (lower images). **c.** Median grain size distribution. The littoral areas are dominated by basaltic blocks and gravel, whereas the profundal areas are characterized by silt/clay fractions that follow the lake bathymetry. **d.** Total organic carbon (TOC) distribution showing two distinct local maxima in the profundal areas and minimum values for all shoreline samples.

0.5 T, and ramp rates during heating and cooling were 30°C min^{-1}. Samples were heated in air to a temperature of ~700°C and subsequently cooled to room temperature (RT), to obtain curves of the induced magnetization (M/M_{RT}).

X-ray diffraction and Fourier transform infrared spectroscopy studies

Prior to X-ray diffraction (XRD) and Fourier transform infrared (FTIR) spectroscopy analyses, magnetic minerals were extracted using ground and sieved sediments. The material was dispersed in double distilled water and flocks were disaggregated by ultrasonic treatment for a short period. After that, the magnetic material in suspension was collected using a magnet and then dried at room temperature. A sample of ~500 mg was collected in order to carry out the analyses.

The major and minor mineral phases in the magnetic extract were identified by XRD, using an automatic Philips PW 3710 X-ray diffractometer with graphite monochromated Cu-Kα radiation ($\lambda = 1.5405$ Å), automatic divergence slit and a scan speed of 0.008° s^{-1}.

The spectroscopic behaviour was analysed by FTIR spectroscopy. These analyses were carried out in order to confirm the diffractometric results and to retrieve information on the mineralogical composition. The samples were previously dried at 100°C within a few hours to eliminate the interference of moisture. Infrared (IR) spectra were recorded on a Nicolet-Magna 550 FTIR instrument with cesium iodide (CsI) optics, using the KBr pellet technique. The source was mid–far IR using a DTGS CsI detector (6400–200 cm^{-1}).

https://doi.org/10.1017/S0954102017000116 Published online by Cambridge University Press

Statistical analyses

Multivariate statistical analysis was performed using the R free software (R version 3.1.3 2015) and aimed to: i) determine the magnetic features of lake sediments and ii) explore the relationship between the magnetic parameters, grain size fractions and TOC. The magnetic parameters used for these analyses were: χ, χ_{ARM}, SIRM and M_s (magnetic concentration dependent parameters), and χ_{ARM}/χ-ratio, χ_{ARM}/SIRM, SIRM/χ, H_c, H_{cr} and the relative contribution of paramagnetic and diamagnetic minerals (magnetic grain size/mineralogy dependent parameters).

The Kruskal–Wallis test was used to determine if there were magnetic differences between grain size fractions. When the Kruskal–Wallis test was significant (i.e. if at least one of the groups is significantly different from at least one of the others) a Conover Inman test (Conover 1999) was performed to analyse differences between the grain size fractions for each magnetic parameter. This is an alternative method of multiple comparisons (its parametric equivalent is the Tukey's range test) that helps to determine which groups are different with appropriately adjusted pairwise comparisons.

The relationships of all of the magnetic parameters was analysed using a principal component analysis (PCA) with matrix correlation. An indicator called Kaiser-Meyer-Olkin (KMO) factor adequacy (Kaiser & Rice 1974) evaluates the appropriateness of applying factor analysis, and a KMO value of <0.5 is considered to advise against applying a PCA. The data matrix was standardized with a column range, and then a correlation matrix was used. The PCA was carried out to study, in a multivariate manner, one-to-one relationships between the variables. The dataset included magnetic and geochemical variables ($n = 45$ samples).

After the PCA, a non-hierarchical k-means cluster analysis (CA) was performed in order to build clusters of samples with similar magnetic, geochemical and grain size features. Each of the clusters is characterized by magnetic variables. The co-ordinates of the rows on the principal components (obtained from PCA) were used to build the clusters. A very high percentage of the inertia ($>80\%$) should be retained by the components selected to obtain a stable and clear hierarchy.

Results

Hydrochemical, grain size and geochemical studies

The main physicochemical characteristics including some trace element concentrations from LA are shown in Table I. Lake Anónima shows particular physicochemical characteristics, with diluted waters (TDS $<100\,mg\,l^{-1}$) that are slightly alkaline with a pH of 7.6 on 17 January 2013 and 8.1 on 12 February 2013. The chemical classification of water bodies on Vega Island is chloride-sodic-potasic. The characteristics of LA are comparable to other lakes from Vega and James Ross islands.

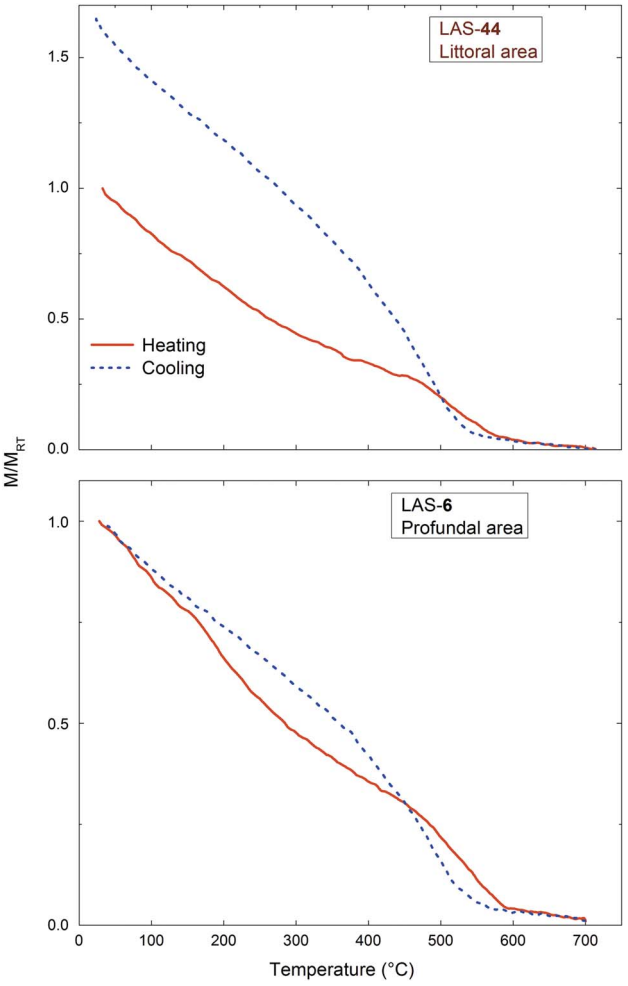

Fig. 4. Thermomagnetic curves for sediment samples corresponding to the littoral and profundal areas of Lake Anónima. Magnetite is the main magnetic mineral with Curie temperatures close to 580°C, and minor secondary magnetic phases with lower Curie temperatures are also visible.

Snow samples were slightly acid (mean pH ~ 6.0) and diluted (mean TDS ~ $11.5\,mg\,l^{-1}$), whereas the stream flowing into the lake is clearly alkaline (pH > 8.0) and more concentrated (TDS ~ $108\,mg\,l^{-1}$). Lake Anónima presents intermediate salinity implicating both sources. This is also shown in Fig. 2a, where the dissolved concentrations of both sources (samples 2N-BD-1/2 and 2R-LA-1) are plotted, and the LA waters (samples 2L-LA-1/2) fall in between snow and river samples. Major element data support this interpretation, as their low concentration in snow samples suggests that water input is supplied by streams and snow meltwater.

https://doi.org/10.1017/S0954102017000116 Published online by Cambridge University Press

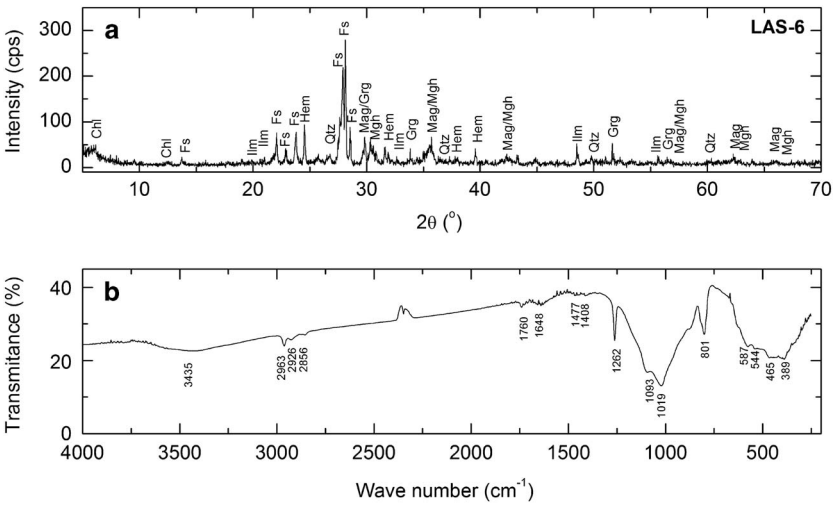

Fig. 5. Magnetic extract (sample LAS-6) from a profundal area in Lake Anónima. **a.** X-ray diffraction spectra indicate the presence of: magnetite (Mag; Fe_3O_4), maghaemite (Mgh; γ-Fe_2O_3), haematite (Hem; α-Fe_2O_3), greigite (Grg; Fe_3S_4), ilmenite (Ilm), quartz (Qtz), feldspar (Fs), chlorite (Chl). **b.** Fourier transform infrared spectra indicate the presence of clays (~3430 cm^{-1}), organic matter (~2960–2860 cm^{-1}, ~1200 cm^{-1}), siliciclastic material (~1020 cm^{-1}), iron oxides (~650–500 cm^{-1}) and iron sulphides (~450 cm^{-1}).

The system also shows significantly dynamic hydrological and hydrochemical behaviour during summer reflected in lake size and water level changes, i.e. an ~20% perimeter decrease (as seen in photos taken in January and February 2013 see Fig. 1d), and by dissolved element concentrations, i.e. different percentage increases. Comparing LA water samples collected on 17 January and 12 February 2013 (Fig. 2b) the corresponding geochemical data show an increase in dissolved element concentration. Perimeter decrease may be caused by infiltration or evaporation processes, but the 14–22% dissolved concentration increases over a short period of time (~1 month) indicate that evaporation dominates over infiltration.

The grain size distribution and percentage of clay (A1), silt (A5, A4, A3 and A2) and sand (B, C and D) in sediment samples is shown in Fig. 3a & c. The TOC content is low due to limited primary productivity (biological communities) in this region (range: 0.40–1.40%, mean: 0.99%, standard deviation: 0.24%) with two distinct local maxima in the deepest areas of the lake (Fig. 3d). Minimum values were detected in all shoreline samples. The TIC content was also low (range: 0.00–0.19%, mean: 0.06%, standard deviation: 0.04%) and therefore these values were discarded and not considered in the statistical analysis. The proportion of TOC was <2.0%; therefore, it is possible to assume that the siliciclastic inorganic fraction (~98.0%) is the main component of the sediment.

Magnetic properties

Curie temperatures were estimated from M(T) curves by the second derivative method and a dominant magnetic phase corresponding to magnetite was revealed for all areas (T_c = 580°C; Fig. 4). In addition, secondary magnetic phases (T_c = 290°C and 690°C) are present and may correspond to iron oxides (e.g. haematite) and iron sulphides (e.g. greigite). The heating curves for samples LAS-6 and LAS-44 are similar, with a slope change between 200°C and 250°C followed by a decrease in magnetization and another slope change at ~500°C with a gradual decay in magnetization to 580°C. The occurrence of ferrimagnetic minerals, such as magnetite and greigite, results in an inflection between 200°C and 300°C, but the marked minimum at ~320°C and the secondary maximum are not observed, and there is a more gradual decay to the Curie temperature of magnetite. Our thermomagnetic curves are not reversible, as the cooling/heating branches show changes in magnetization M(T) after heating. As observed in Fig. 4, the littoral sample (LAS-44) shows a magnetization increase of ~70% with respect to the M_{RT} after cooling, which points to the formation of new ferrimagnetic minerals.

The XRD patterns for sample LAS-6 from a profundal site are shown in Fig. 5a. Magnetic minerals as interpreted above from thermomagnetic studies are supported by magnetite, haematite and greigite peaks. In addition, the FTIR spectrum of the magnetic extract is shown in Fig. 5b. The spectrum shows minima wave numbers corresponding to different mineral groups, e.g. iron oxides (~650–500 cm^{-1}), iron sulphides (~450 cm^{-1}) and OM (~2960–2860 cm^{-1}, ~1200 cm^{-1}), among others. It is worth mentioning that the presence of OM should not be expected in this magnetic extract because OM would produce a diamagnetic signal and because of the previous ultrasonic disaggregation of the sediments in suspension. This

https://doi.org/10.1017/S0954102017000116 Published online by Cambridge University Press

Table II. Collection sites, magnetic parameters, total organic carbon (TOC) and grain size analyses of sediment samples from Lake Anónima, Vega Island.

Sample	Depth m	UTM East m	UTM North m	χ 10^{-8} m^3 kg^{-1}	SIRM 10^{-3} Am^2 kg^{-1}	χ_{ARM} 10^{-8} m^3 kg^{-1}	M_s 10^{-3} Am^2 kg^{-1}	χ_{ARM}/χ	χ_{ARM}/SIRM 10^{-5} m A^{-1}	SIRM/χ kA m^{-1}	H_c mT	H_{cr} mT	Para/diamag. cont. %[a]	TOC %	Size µm Median	Size µm Mean
LAS-1	0.0	483970.77	2922728.39	63.8	41.8	774.3	83.7	12.1	18.5	65.5	28.5	36.4	65.6	0.651	952.3	890.5
LAS-2	0.0	483971.53	2922728.76	70.0	33.9	836.8	182.3	11.9	24.7	48.4	25.4	48.3	38.5	0.599	948.9	946.8
LAS-3	0.0	483972.3	2922729.13	72.5	37.2	813.1	123.2	11.2	21.9	51.3	26.0	51.5	26.1	0.789	167.9	269.9
LAS-4	0.0	483973.06	2922729.5	97.8	62.2	1265.2	151.1	12.9	20.3	63.6	27.9	44.1	26.6	0.403	345.7	705.8
LAS-5	2.9	484009.05	2922761.01	123.8	58.2	1233.8	169.4	10.0	21.2	47.0	24.9	54.2	32.4	1.012	12.8	22.7
LAS-6	3.2	484008.53	2922766.58	115.5	55.3	1020.8	198.3	8.8	18.5	47.9	24.5	36.8	22.2	1.156	15.6	54.6
LAS-7	3.4	484009.48	2922773.27	106.7	56.6	955.5	138.9	9.0	16.9	53.0	24.6	52.3	32.9	1.404	15.3	31.4
LAS-8	2.7	484010.44	2922776.62	100.1	57.1	1014.4	171.5	10.1	17.8	57.0	26.0	46.4	19.1	1.101	24.1	49.2
LAS-9	2.7	484003.19	2922741.92	113.1	65.6	1042.7	174.6	9.2	15.9	58.0	24.2	55.3	36.8	1.045	16.6	24.3
LAS-10	3.2	484002.27	2922737.57	109.8	50.7	994.8	171.9	9.1	19.6	46.2	22.6	48.3	23.8	1.175	20.0	37.8
LAS-11	2.3	484000.33	2922733.1	88.2	43.3	801.0	134.8	9.1	18.5	49.1	24.9	53.1	43.5	1.181	50.4	62.4
LAS-12	3.0	484010.54	2922757.67	119.2	59.4	1090.3	194.5	9.1	18.4	49.8	23.7	51.6	24.3	1.167	14.2	24.9
LAS-13	3.3	484012.96	2922755.35	109.0	55.7	982.9	170.2	9.0	17.6	51.1	23.9	51.1	36.3	1.293	16.9	33.9
LAS-14	2.8	484002.66	2922758.75	109.2	58.6	982.3	179.9	9.0	16.8	53.7	24.3	53.3	31.9	1.313	14.6	23.8
LAS-15	1.8	484001.16	2922763.2	110.6	50.8	1015.3	174.4	9.2	20.0	45.9	24.8	42.7	35.3	0.857	37.2	166.7
LAS-16	2.8	484014.44	2922764.38	105.2	48.1	928.3	161.6	8.8	19.3	45.7	23.9	53.2	35.4	0.990	25.3	37.3
LAS-17	3.1	484013.48	2922759.92	99.9	60.9	1060.9	168.7	10.6	17.4	61.0	24.0	49.6	33.4	1.235	16.6	32.9
LAS-18	2.6	484006.62	2922754.31	107.1	63.8	1013.3	179.1	9.5	15.9	59.6	23.4	44.6	30.7	1.191	18.7	36.0
LAS-19	3.8	483998.78	2922746.47	117.1	56.5	971.4	172.8	8.3	17.2	48.2	23.9	51.8	33.2	0.952	21.1	33.8
LAS-20	4.1	483991.42	2922741.98	114.0	59.9	1061.0	184.9	9.3	17.7	52.5	24.2	51.8	30.1	1.052	18.9	31.4
LAS-21	2.4	483988.97	2922739.73	88.1	55.3	1165.9	230.5	13.2	21.1	62.8	28.8	51.6	32.5	0.554	138.5	250.5
LAS-22	0.8	483985.06	2922734.14	87.4	52.8	1029.8	103.7	11.8	19.5	60.4	23.6	41.9	54.9	0.617	96.4	125.5
LAS-23	0.7	483982.6	2922734.13	93.7	50.7	988.3	139.2	10.6	19.5	54.1	24.1	44.8	30.5	1.035	83.6	185.2
LAS-24	2.4	484001.14	2922767.65	111.2	55.0	999.9	142.5	9.0	18.2	49.5	24.6	51.8	37.9	1.164	23.2	37.5
LAS-25	2.5	484003.13	2922763.21	107.4	54.7	1013.8	175.8	9.4	18.5	50.9	23.6	53.7	33.5	1.208	14.0	31.2
LAS-26	2.8	484007.1	2922756.54	117.5	56.3	1041.3	170.9	8.9	18.5	47.9	24.2	43.5	35.5	1.180	14.7	26.1
LAS-27	2.5	484006.64	2922749.85	112.7	57.9	1038.3	179.7	9.2	17.9	51.4	24.4	49.4	33.5	0.986	24.8	45.4
LAS-28	2.9	484001.77	2922739.8	112.2	57.6	1037.9	170.7	9.3	18.0	51.3	23.3	50.0	34.2	1.117	21.1	31.0
LAS-29	3.5	483997.83	2922740.89	106.1	44.0	950.9	160.5	9.0	21.6	41.5	23.6	38.4	37.3	1.241	19.3	30.9
LAS-30	2.8	483986.97	2922746.41	86.9	52.8	649.3	155.0	7.5	12.3	60.8	22.2	48.9	29.4	1.361	60.8	198.0
LAS-31	1.7	483984.02	2922745.28	99.7	49.6	995.6	171.6	10.0	20.1	49.7	24.6	51.5	34.5	0.883	60.6	173.5
LAS-32	3.1	484012.92	2922773.29	75.1	43.3	748.3	97.3	10.0	17.3	57.7	25.4	43.5	66.8	1.145	88.8	219.5
LAS-33	3.0	484010.98	2922767.7	119.1	61.7	1146.1	162.1	9.6	18.6	51.8	24.1	52.9	38.6	1.160	16.2	25.9
LAS-34	3.1	484001.73	2922747.6	108.4	59.7	1022.9	166.4	9.4	17.1	55.1	23.9	52.2	38.0	0.981	21.0	37.1
LAS-35	2.0	483996.38	2922735.31	85.5	45.5	871.8	123.9	10.2	19.2	53.2	29.3	47.1	52.0	0.872	82.2	140.5
LAS-36	0.4	483993.43	2922735.3	87.1	37.3	798.6	115.8	9.2	21.4	42.8	27.0	45.1	51.8	0.892	99.9	206.4
LAS-37	0.8	483986.99	2922741.95	86.9	47.2	1109.4	149.7	12.8	23.5	54.3	23.0	49.0	27.0	0.714	96.4	198.9
LAS-38	3.1	483990.89	2922750.89	108.4	60.8	1014.7	183.5	9.4	16.7	56.1	22.5	46.1	26.8	1.098	23.3	36.4
LAS-39	2.2	484000.2	2922758.73	127.8	66.6	1282.2	195.2	10.0	19.3	52.1	25.3	54.9	33.7	0.989	11.1	18.7
LAS-40	3.4	483996.79	2922752.03	118.0	58.2	1122.1	190.9	9.5	19.3	49.3	23.5	49.4	27.6	0.970	17.3	25.4
LAS-41	3.8	483995.82	2922747.57	111.6	47.1	1059.9	186.9	9.5	22.5	42.2	23.7	41.9	30.8	1.113	19.0	30.4
LAS-42	2.8	484002.2	2922753.17	116.4	52.0	1123.8	180.2	9.7	21.6	44.7	24.0	49.7	27.2	0.924	16.2	28.0
LAS-43	0.0	483981.16	2922727.44	76.5	37.6	926.4	121.5	12.1	24.6	49.2	27.5	38.8	50.3	0.532	250.0	478.3
LAS-44	0.0	483986.07	2922730.8	86.9	42.6	990.7	114.1	11.4	23.3	49.0	30.6	42.7	38.2	0.586	280.4	521.0
LAS-45	0.0	483990.01	2922728.6	90.0	38.4	890.9	123.2	9.9	23.2	42.7	26.4	41.4	50.6	0.679	88.8	200.4
Mean	2.2			101.6	52.5	997.3	159.9	9.9	19.3	51.9	24.9	47.9	35.8	0.990	98.2	151.5
SD	1.2			15.6	8.3	130.4	30.2	1.3	2.5	5.9	1.9	5.1	10.3	0.244	200.0	221.7
Min.	0.0			63.8	33.9	649.3	83.7	7.5	12.3	41.5	22.2	36.4	19.1	0.403	11.1	18.7
Max	4.1			127.8	66.6	1282.2	230.5	13.2	24.7	65.5	30.6	55.3	66.8	1.404	952.3	946.8

[a]Relative contribution of paramagnetic and diamagnetic minerals.

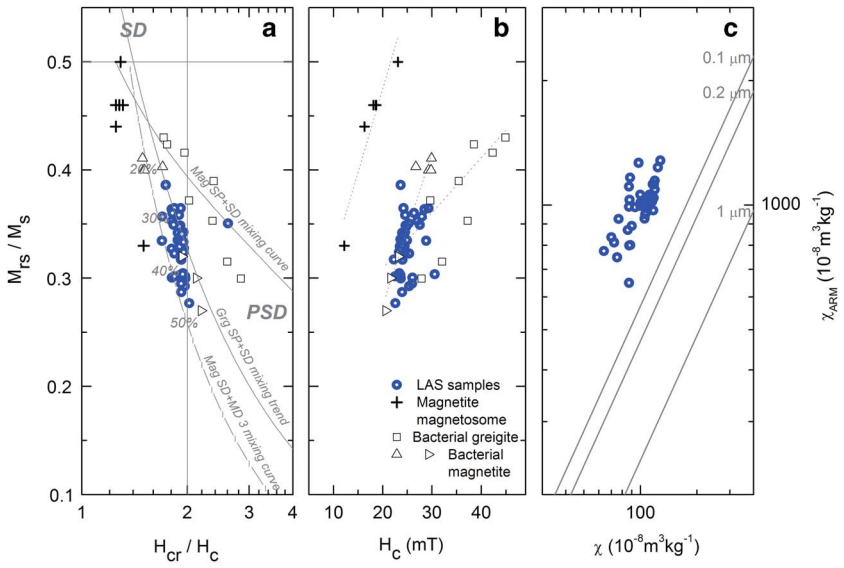

Fig. 6. Magnetic granulometry for sediment from Lake Anónima. **a.** Day plot with domain state regions and mixing lines for SD + MD and SP + SD mixtures of magnetite (Mag; modified from Dunlop 2002), and mixing trend for SP + SD mixtures of greigite (Grg; Roberts *et al.* 2011). **b.** Biplot of H_c *vs* M_{rs}/M_s with the dotted lines indicating the trend for magnetite magnetosome (Fischer *et al.* 2008, Li *et al.* 2010), bacterial magnetite in lake sediments (triangles: Snowball 1994, triangles pointing right: Pan *et al.* 2005) and bacterial greigite in laminated sapropels (Reinholdsson *et al.* 2013). **c.** χ *vs* χ_{ARM} variation for sediment samples from Lake Anónima with lines of constant grain size of magnetite minerals (King *et al.* 1982). MD = multidomain, PSD = pseudo-single-domain, SD = single-domain, SP = superparamagnetic.

suggests that the observed OM must be associated with the magnetic minerals.

These results confirm the dominance of ferrimagnetic minerals as interpreted from IRM studies (Table II). H_{cr} was characteristic of magnetite and greigite minerals at 36.4–55.3 mT (mean: 47.9 ± 5.1 mT). In addition, SIRM/χ ranged between 41.9–67.8 kA m^{-1}, such high values may indicate the presence of greigite (SIRM/χ > 40 kA m^{-1}) and/or very fine magnetite. The S-ratio indicates the relative presence of ferrimagnetic (e.g. magnetite, titanomagnetite, maghaemite or greigite) versus antiferromagnetic materials (e.g. haematite or goethite). The sediment sample from LA have S-ratio values close to 0.90, corresponding to the predominance of ferrimagnetic minerals.

Magnetic hysteresis results (Table II) are represented in the Day plot and show that magnetite and greigite tend towards the single-domain (SD) size region (Fig. 6a). The LA data lie between mixing curves for SD + MD (multidomain) mixtures of magnetite (mixing curve 3) and for SD + SP (superparamagnetic) mixtures of greigite (mixing trend). The χ_{ARM}/χ-ratio is a grain size sensitive parameter, with values of $\chi_{ARM}/\chi > 5$ indicating the presence of magnetite grains of ≤ 0.1 μm (Peters & Dekkers 2003), which is also observed on the King's plot (Fig. 6c).

Statistical classification of sediment samples

Grain size analysis indicated variations in mean, median and mode values, thus the sediments were classified into four granulometric groups: coarse–medium sand D ($n = 6$), fine–very fine sand C–B ($n = 8$), coarse–medium silt A5–A4 ($n = 17$) and fine–very fine silt A3–A2 ($n = 14$).

Table III. Multivariate comparison test after Kruskal–Wallis test. The granulometric groups for sediments are: coarse–medium sand D (>250 μm), fine–very fine sand C–B (63–250 μm), coarse–medium silt A5–A4 (15.8–63 μm) and fine–very fine silt A3–A2 (3.9–15.6 μm). TRUE indicates that differences are larger than a critical value at the significance level of $P = 0.05$.

Grain size group	Magnetic parameters					Geochemical variables		Lake characteristics
	χ	SIRM	M_s	χ_{ARM}/χ	χ_{ARM}/SIRM	H_c	TOC	Depth
C–B and D	False	False	False	False	False	False	False	False
C–B and A3–A2	TRUE	TRUE	TRUE	False	False	False	TRUE	TRUE
C–B and A5–A4	TRUE	False	False	False	False	False	False	TRUE
D and A3–A2	TRUE	TRUE	TRUE	TRUE	TRUE	TRUE	TRUE	TRUE
D and A5–A4	TRUE	False	False	TRUE	TRUE	TRUE	TRUE	TRUE
A3–A2 and A5–A4	False	False	False	False	False	False	False	False

https://doi.org/10.1017/S0954102017000116 Published online by Cambridge University Press

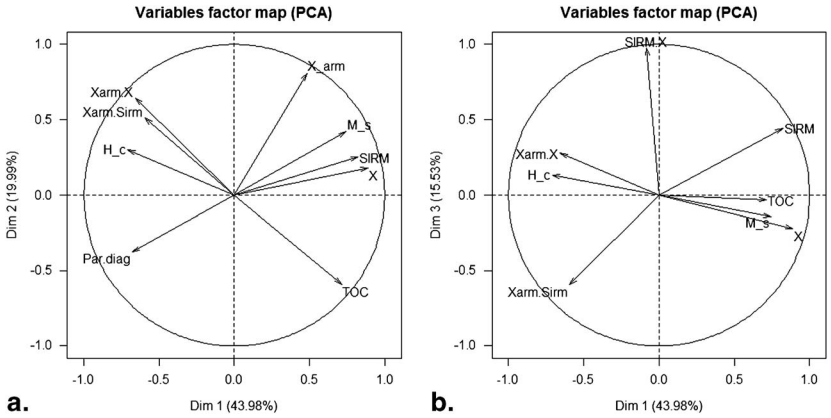

Fig. 7. Principal component analysis (PCA) for Lake Anónima using magnetic and physicochemical variables. The PCA biplots show **a.** a direct relationship between χ, M_s and SIRM with total organic carbon (TOC) and **b.** an inverse relationship between χ_{ARM}/χ, H_c and χ_{ARM}/SIRM with TOC.

A Kruskal–Wallis test was performed to determine if there are differences in magnetic properties between these four groups. A non-parametric test was used because the normality assumption was rejected (Shapiro–Wilk's test) for all magnetic variables. The results show that there are significant differences ($P < 0.05$) between fraction groups using magnetic concentration dependent variables (χ, SIRM and M_s), magnetic grain size dependent variables (χ_{ARM}/χ and χ_{ARM}/SIRM) and magnetic mineralogy dependent variables (H_c). Significant between-group differences were also seen for TOC and water depth ($P < 0.05$) (Table III).

After testing the contribution of magnetic and geochemical variables which show significant differences between groups, a multiple comparison test was performed (Table III). For all variables, there were no significant differences ($P < 0.05$) between groups D and C–B and between groups A5–A4 and A3–A2. However, there were significant differences between C–B and A3–A2 (χ, SIRM, M_s, TOC, depth), C–B and A5–A4 (χ, depth), D and A3–A2 (χ, SIRM, M_s, χ_{ARM}/χ, χ_{ARM}/SIRM, H_c, TOC, depth), and D and A5–A4 (χ, χ_{ARM}/χ, χ_{ARM}/SIRM, H_c, TOC, depth). This result is interesting since it can be inferred that the clear differences in magnetic properties between these groups is related to the sand and silt fractions.

The KMO factor adequacy is 0.68, which indicates that it is appropriate to perform a PCA. The analysis yields a 79.5% variance explained by three principal components. The biplot shows an inverse relationship between χ_{ARM}/χ, χ_{ARM}/SIRM and H_c with TOC (Fig. 7a) and a direct relationship between the magnetic parameters χ, SIRM and M_s with TOC (Fig. 7b). There is a direct relationship between magnetic parameters of the same 'magnetic category' (i.e. concentration, size or mineralogy). The magnetic concentration dependent parameters χ, SIRM and M_s have an inverse relationship with parameters of the paramagnetic/diamagnetic contribution.

From this PCA result, a CA was performed using the magnetic variables in order to determine clusters of samples with similar magnetic features. As complementary information, the four grain size groups (D, C–B, A5–A4 and A3–A2) were used as additional variables. This way, the optimal partition of samples yielded two groups: cluster 1 composed of 13 samples of groups D ($n = 6$), C–B ($n = 6$) and A5–A4 ($n = 1$), and

Table IV. Clusters of samples with similar magnetic features obtained from a non-hierarchical k-means cluster analysis.

Variable	Mean overall	Cluster 1 (n = 13) D (n = 6), C–B (n = 6), A5–A4 (n = 1)		Cluster 2 (n = 32) C–B (n = 2), A5–A4 (n = 16), A3–A2 (n = 14)	
		Mean group	P-value	Mean group	P-value
χ (10^{-8} m^3 kg^{-1})	101.6	82.1	4.9E-07	109.6	8.5E-08
SIRM (10^{-3} Am^2 kg^{-1})	52.5	44.2	3.5E-06	55.8	2.6E-05
M_s (10^{-3} Am^2 kg^{-1})	159.9	132.3	2.1E-04	171.1	9.1E-05
χ_{ARM}/χ	9.9	11.4	2.4E-04	9.3	4.9E-07
χ_{ARM}/SIRM (10^{-5} m A^{-1})	19.3	21.4	7.0E-03	18.4	2.1E-04
H_{cr} (mT)	47.9	44.7	9.1E-05	49.2	7.1E-03
H_c (mT)	24.9	26.9	2.6E-05	24.0	3.5E-06
Para/diamagnetic contribution (%)	35.8	44.7	2.2E-07	32.2	2.4E-04
Total organic carbon (%)	0.99	0.70	8.5E-08	1.11	2.2E-07

https://doi.org/10.1017/S0954102017000116 Published online by Cambridge University Press

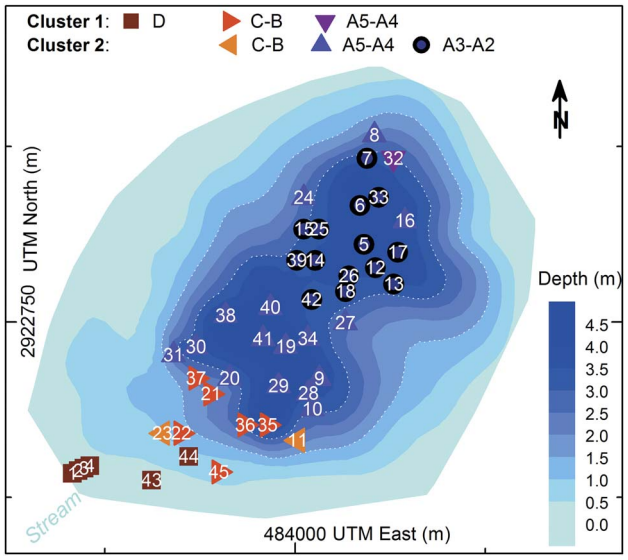

Fig. 8. Cluster analysis results for magnetic parameters and total organic carbon. There are two clusters of samples of coarse–fine sand fractions (cluster 1) and coarse–fine silt fractions (cluster 2).

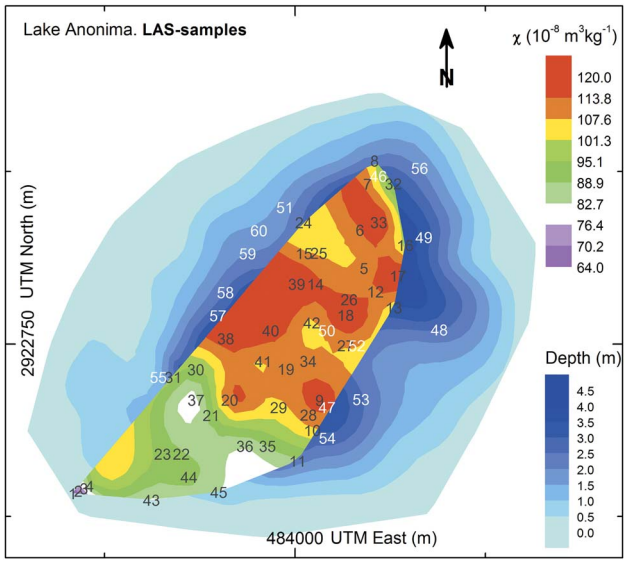

Fig. 9. Distribution of magnetic susceptibility χ as a concentration parameter. The highest values are observed in profundal areas. Note the influence of a stream developing a delta on the south-west coast.

cluster 2 composed of 32 samples of groups C–B ($n = 2$), A5–A4 ($n = 16$) and A3–A2 ($n = 14$).

All variables used for the CA provide meaningful information for the partition of both clusters and are presented in Table IV. The samples corresponding to sand fractions (D and C–B, cluster 1) and silt fraction (A5–A4 and A3–A2, cluster 2; Table IV) are clearly differentiated in Fig. 8. Magnetic concentration dependent parameters characterize both clusters clearly; higher values are obtained for cluster 2. Regarding the magnetic mineralogy, cluster 1 has relatively finer magnetic grains than cluster 2, and relatively softer magnetic contribution (lower H_{cr} values) of ferrimagnetic minerals. In addition, the highest TOC values were observed in the cluster dominated by silt fractions (cluster 2).

Discussion

Ferrimagnetic minerals in Lake Anónima

The ferrimagnetic minerals identified in LA sediments may occur as primary detrital particles from volcanic rocks and as secondary minerals. Both components possibly coexist, but in general, sedimentary particles of primary origin are dominantly pseudo-single-domain (PSD) and MD (with grain sizes > 1 μm). Smaller iron oxides (SP and SD particles) may be of primary origin and they are mostly embedded in host silicates (Ludwig *et al.* 2013). On the other hand, secondary ferrimagnetic minerals (such as magnetite and greigite) can form via bacterial assimilatory and dissimilatory processes, or purely inorganically as products of early diagenesis (Roberts *et al.* 2011, Lascu & Plank 2013). Such secondary ferrimagnetic particles in sediments are mostly SP and SD at room temperature (Ludwig *et al.* 2013). The magnetic analysis in LA reveals the dominance of SD ferrimagnetic minerals, which is in agreement with results obtained in sediment cores from lakes Buena and Roja, James Ross Archipelago, with similar physicochemical characteristics (Lecomte *et al.* 2016). These lacustrine systems are located over glacial deposits with both local sedimentary (Cretaceous rocks) and volcanic (Tertiary volcanic rocks) composition. However, processes occurring in these lakes are associated with physicochemical changes (diagenesis of original minerals) and biological activity (cyanobacteria and algal photosynthesis; Nedbalova *et al.* 2013) and they seem to produce different magnetic minerals. Among these minerals, iron sulphides (greigite) and iron oxides (magnetite and haematite) are identified not only by thermomagnetic studies and relevant magnetic parameters (e.g. H_{cr}, SIRM/χ), but also by XRD and FTIR studies (Fig. 5).

Magnetite is characterized by high magnetic stability and fine magnetic grain size (< 0.1 μm, SD grains), similar to lake sediments where bacterial magnetite has been reported (Snowball 1994, Pan *et al.* 2005). A comparison of the magnetic domains and grain size studies for LA sediment and other lakes with bacterial magnetite and greigite is displayed in Fig. 6a & b. The presence of such biogenic ferrimagnetic minerals in LA is supported by the following arguments: i) the positive relationship between

https://doi.org/10.1017/S0954102017000116 Published online by Cambridge University Press

magnetic parameters with TOC, as also found in Swedish lake sediments (Snowball *et al.* 2002), in Swiss and Russian lake sediments (Egli 2004) and in North American lake sediments (Lascu & Plank 2013), and ii) the presence of OM probably associated with iron oxides as observed by FTIR spectrum in magnetic extracts (Fig. 5b). Moreover, the presence of magnetotactic bacteria (MTB), which synthesize high quality SD magnetite crystals (magnetosomes), may also be possible according to a recent study on lake sediments from Vega Island (Coria *et al.* 2015) where the MTB species *Magnetospirillum magnetotacticum* was identified from its protein *mam*A (magnetosome associated TPR-containing protein) using the nested polymerase chain reaction process.

Depositional environments

The littoral areas of the lake are dominated by basaltic blocks and gravel (Fig. 3b), whereas the deepest regions are characterized by silt/clay fractions that follow the lake bathymetry (Fig. 3c) In particular, the sand fractions are restricted to the south-west coast and are associated with the main stream and the development of a small delta (Fig. 3b). The CA, using meaningful magnetic parameters, grain size and TOC results in two clusters of samples that involve coarse–fine sand facies (cluster 1) and coarse–fine silt facies (cluster 2) allowing the definition of two principal recent depositional sub-environments in LA: i) the shoreline and littoral region and ii) the profundal or distal areas.

Such sub-environments are directly influenced by the dynamics of the main stream located in the south-west lake basin, the lake bottom morphology and the dynamic hydrological behaviour during summer as indicated by water level and shoreline contour changes (Fig. 1c). In addition, intense winds in this region generate strong wave action and it is assumed that this may provide an important influx of sediments (i.e. silt fraction) into the lake. Compositionally, the sediments in both sub-environments are dominated by siliciclastic material (~98.0%), whereas the non-siliciclastic material (< 2.0%), dominated by OM (expressed as TOC), is mainly restricted to the deeper parts of the lake. The key spatial grain size characteristic of the lake sediments is not uniform in a direction parallel to the shoreline, but changes progressively from coarse to fine grains from the south-western shore towards the deepest areas (Figs 3a & 8). If complementary information regarding grain size composition is analysed it is possible to define two further sub-areas for each cluster. Cluster 1 can be divided into a deltaic area (a1) and a littoral area (a2), and cluster 2 can be divided into southern (b1) and northern (b2) profundal areas (see Fig. 8). There is a littoriprofundal transition area, not defined by the CA, that is characterized by the transition between coarse and fine sediments. These four sub-areas are summarized as follows.

The littoral area (a2) is characterized by the predominance of basaltic blocks and gravel, and steep slopes around the lake (see Fig. 3b). This region shows a high energy sedimentary environment, with particle entrainment occurring due to the action of waves and wave energy coupled with gravitational instability on a steeper slope. The deltaic area (a1) (predominantly made of sand), which is a relatively flat region restricted to the south-west part of the lake system, developed by the surface main stream inflow and sediment input, and is influenced by lake level fluctuations during summer and important wave dynamics. Such a dynamic behaviour in this sub-environment promotes the resuspension of finer clay–silt fractions to quieter areas (profundal accumulation areas). In cluster 1, a coarse sand fraction D is deposited near the coastline (a2) and fine sand fractions C–B prevail in the deltaic area (a1). These areas show a lower concentration of magnetic minerals and TOC content (Table IV, Figs 3d & 9).

The profundal areas comprise the central and deepest parts of the lake. It is characterized by predominance of fine sediments, i.e. coarse silt fraction A5–A4 and fine silt fraction A3–A2. In this area, two depocenters were recognized with maximum water depths of 4.2 (southern profundal area, b1) and 4.6 m (northern profundal area, b2). Finer sediments are transported to these central zones due to a low energy sedimentary environment, whereas coarser grains are retained in shallower zones. The granulometric characteristics indicate that finer silt sediments (A3–A2) are deposited in the northern profundal area.

Consequently, the shoreline and littoral areas can be considered as regions of redistribution, erosion and transport, while profundal areas can be mainly considered as sediment accumulation areas.

Consideration of transport and depositional processes represented by the partitioned grain size components help to characterize changes in sedimentary sub-environments and thus enable the characterization of the spatial distribution. Variation trends of the clastic components indicate good correlations with observed magnetic properties. The magnetic concentration dependent parameters SIRM, M_s and χ indicate variable concentrations of ferrimagnetic material across the lake bottom (Fig. 9). The profundal areas of LA are characterized by higher concentrations of ferrimagnetic particles, in particular, such sediments show the highest values of magnetic concentration dependent parameters χ (109.6×10^{-8} m^3 kg^{-1}), M_s (171.1×10^{-3} Am^2 kg^{-1}), SIRM (55.8×10^{-3} Am^2 kg^{-1}), TOC (1.11%) and the magnetic mineralogy dependent parameter H_{cr} (49.2 mT), while the shoreline and littoral sediments show the lowest values for these parameters, i.e. $\chi = 82.1 \times 10^{-8}$ m^3 kg^{-1}, $M_s = 132.3 \times 10^{-3}$ Am^2 kg^{-1}, SIRM $= 44.2 \times 10^{-3}$ Am^2 kg^{-1},

https://doi.org/10.1017/S0954102017000116 Published online by Cambridge University Press

TOC = 0.70%, and H_{cr} = 44.2 mT. The spatial distribution of median grain size, TOC and χ represented in Figs 3c, 3d, 8 & 9 show the influence of the stream that has developed a delta near the south-west coast of LA.

Thus, knowledge about the spatial distribution and control of magnetic properties and non-magnetic sedimentological components in this Antarctic lake provides a basis for new studies focusing on past environmental and climate changes using sedimentary sequences in this lake and areas at these latitudes.

Conclusions

Hydrological behaviour of LA results in strong lake level fluctuations during the summer, which may produce changes in sediment input and redistribution in the bottom of the lake. It presents a marked seasonal evolution, occurring during a short time interval of ~1 month, producing a reduction in the lake level and an increase in most dissolved elements. The main stream located on the south-west coast of the lake, basin morphology, water depths and the dynamic hydrological/hydrochemical behaviour during summer are the main factors controlling the distribution of the present-day surface sediments in this lacustrine system. Magnetic, geochemical and grain size variables indicate probable resuspension of littoral sediment due to sudden lake level changes during the summer followed by redistribution and accumulation in the deepest areas of the lake.

The magnetic signal of the LA sediments is dominated by ferrimagnetic minerals, such as magnetite and greigite, identified by thermomagnetic curves, magnetic hysteresis plots, relevant magnetic parameters (SIRM/$\chi = 51.9 \pm 5.9$ kA m^{-1} and $H_{cr} = 47.9 \pm 5.1$ mT), and non-magnetic analyses including XRD and FTIR. Ferrimagnetic minerals seem to occur as primary detrital particles from volcanic rocks and as secondary minerals. Processes occurring in this lake are associated to diagenesis of original minerals and may also involve biological activity producing secondary magnetic minerals. The relationship between magnetic minerals with OM and its presence in magnetic extracts used for FTIR suggest the presence of biogenic ferrimagnetic minerals, although further studies are needed for confirmation. Ultra-fine ferrimagnetic minerals of SD grain size (< 0.1 μm) are present as indicated by χ_{ARM}/χ values of 9.9 ± 1.3, and seem to be dominant in LA with higher concentration (e.g. $\chi = 101.6 \pm 15.6 \times 10^{-8}$ m^3 kg^{-1} and SIRM = $52.5 \pm 8.3 \times 10^{-3}$ Am^2 kg^{-1}) relative to other lakes on Vega Island.

Results from the Kruskal–Wallis tests using magnetic variables (χ, SIRM, M_s, χ_{ARM}/χ, χ_{ARM}/SIRM and H_c), variables TOC and depth show significant ($P < 0.05$) differences between four granulometric groups. Meaningful magnetic parameters and non-magnetic variables are separated by PCA. The CA identified two clusters of samples that involve deposition areas with coarse–fine sand facies (cluster 1) and coarse–fine silt facies (cluster 2), which defines two main recent depositional sub-environments in LA. The grain size distribution is useful to discriminate between the high energy areas (dominated by sand deposits from the main stream) and the low energy areas located in the interior of the lake (silt and clay fractions). In addition, these two clusters can be further divided by grain size, identifying four sub-environments in LA: deltaic area (a1), littoral area (a2), southern profundal area (b1) and northern profundal area (b2).

The characterization of recent lacustrine sediments present in LA is an important step towards understanding the geochemical and environmental processes occurring in Antarctic ecosystems. Thus, the sedimentological, geochemical and magnetic changes observed in LA sediments contribute to our understanding of the present-day lacustrine dynamic and sedimentary processes, and this information may be used for reconstructing past climates from lake sediment cores in the Antarctic region.

Acknowledgements

The authors wish to thank UNCPBA, UNC and UNAM, DNA, and Consejo Nacional de Investigaciones Científicas y Técnicas (CONICET) for their financial support. They also thank Ing. J. Escalante (Tech. CGEO-UNAM) and P. Zubeldia (Tech. CICPBA). The authors thank the Editor and two anonymous reviewers whose comments greatly improved the manuscript. This contribution was supported by the ANPCYT project PICTO-2010-0096 and by the Bilateral CONICET/CONACYT Project No. 207149 (Harald Böhnel) and Res. 1001/14-5131/15 (Marcos Chaparro).

Author contribution

Marcos Chaparro led the project and the sampling Antarctic campaign CAV-2012/2013, carried out magnetic measurements and was primarily responsible for data analysis and writing the manuscript. Mauro Chaparro and Francisco Córdoba participated in the sampling campaign, contributed to the manuscript preparation, made statistical analyses (MC) and analysed grain size/geochemical data (FC). Karina Lecomte contributed to the manuscript preparation, processed and discussed the hydrochemical and geochemical measurements. José Gargiulo and Nadia Manograsso Czalbowski partook in the sampling campaign, prepared sediment samples, carried out magnetic measurements (JG) and contributed with geological data (NMC). Ana Barrios and Araceli Lavat prepared magnetic extracts of sediment samples, carried out the XRD and FTIR studies and discussed the results. Gimena Urán prepared sediment

samples for grain size and geochemical measurements and processed these results. Harald Böhnel contributed to manuscript preparation and data analysis.

References

Alfonso, J.A., Vasquez, Y., Hernandez, A.C., Mora, A., Handt, H. & Sira, E. 2015. Geochemistry of recent lacustrine sediments from Fildes Peninsula, King George Island, Maritime Antarctica. *Antarctic Science*, **27**, 462–471.

Björck, S., Olsson, S., EllisEvans, C., Håkansson, H., Humlum, O. & deLirio, J.M. 1996. Late Holocene palaeoclimatic records from lake sediments on James Ross Island, Antarctica. *Palaeogeography Palaeoclimatology Palaeoecology*, **121**, 195–220.

Chaparro, M.A.E., Nuñez, H., Lirio, J.M., Gogorza, C.G.S. & Sinito, A.M. 2007. Magnetic screening and heavy metal pollution studies in soils from Marambio Station, Antarctica. *Antarctic Science*, **19**, 379–393.

Chaparro, M.A.E., Gargiulo, J.D., Irurzun, M.A., Chaparro, M.A.E., Lecomte, K.L., Böhnel, H.N., Córdoba, F.E., Vignoni, P.A., Manograsso Czalbowski, N.T., Lirio, J.M., Nowaczyk, N.R. & Sinito, A.M. 2014. El uso de parámetros magnéticos en estudios paleolimnológicos en Antártida. *Latin American Journal of Sedimentology and Basin Analysis*, **21**, 77–96.

Conover, W.J. 1999. *Practical nonparametric statistics*, third edition. New York, NY: Wiley, 596 pp.

Coria, S.H., López, J.L., Lirio, J.M., Vignoni, P.A., Kopalová, K., Lecomte, K.L., Gargiulo, J.D., Chaparro, M.A.E., Vázquez, S., Dionisi, H.M., Lozada, M. & MacCormack, W.P. 2015. *Detección de secuencias correspondientes al gen* mam*A en sedimentos Antárticos marinos y lacustres*. Proceedings of the III Congreso Argentino de Microbiología Ambiental y Agrícola, Buenos Aires. Available at: https://www.researchgate.net/publication/295919952_DETECCION_DE_SECUENCIAS_CORRESPONDIENTES_;AL_GEN_mamA_EN_SEDIMENTOS_ANTARTICOS_MARINOS_Y_LACUSTRES.

Dean, W.E. 1974. Determination of carbonate and organic matter in calcareous sediments and sedimentary rocks by loss on ignition: comparison with other methods. *Journal of Sedimentary Petrology*, **44**, 242–248.

Dean, W.E. 1999. The carbon cycle and biogeochemical dynamics in lake sediments. *Journal of Paleolimnology*, **21**, 375–393.

Dunlop, D. 2002. Theory and application of the Day plot (M_{rs}/M_s versus H_{cr}/H_c) 1. Theoretical curves and tests using titanomagnetite data. *Journal of Geophysics Research - Solid Earth*, 10.1029/2001JB000486.

Egli, R. 2004. Characterization of individual rock magnetic components by analysis of remanence curves. 1. Unmixing natural sediments. *Studia Geophysica et Geodaetica*, **48**, 391–446.

Ermolin, E., De Angelis, H. & Skvarca, P. 2002. Mapping of permafrost on Vega Island, Antarctic Peninsula, using aerial photography and satellite image. *Annals of Glaciology*, **34**, 184–188.

Fischer, H., Mastrogiacomo, G., Loeffler, J.F., Warthmann, R.J., Weidler, P.G. & Gehring, A.U. 2008. Ferromagnetic resonance and magnetic characteristics of intact magnetosome chains in *Magnetospirillum gryphiswaldense*. *Earth Planetary Science Letters*, **270**, 200–208.

Hawes, I., Howard-Williams, C. & Sorrell, B. 2014. Decadal timescale variability in ecosystem properties in the ponds of the McMurdo Ice Shelf, southern Victoria Land, Antarctica. *Antarctic Science*, **26**, 219–230.

Heiri, O., Lotter, A.F. & Lemcke, G. 2001. Loss on ignition as a method for estimating organic and carbonate content in sediments: reproducibility and comparability of results. *Journal of Paleolimnology*, **25**, 101–110.

Hodgson, D.A., Roberts, S.J., Smith, J.A., Verleyen, E., Sterken, M., Labarque, M., Sabbe, K., Vyverman, W., Allen, C.S., Leng, M.J. & Bryant, C. 2013. Late Quaternary environmental changes in Marguerite Bay, Antarctic Peninsula, inferred from lake sediments and raised beaches. *Quaternary Science Reviews*, **68**, 216–236.

Kaiser, H.F. & Rice, J. 1974. Little jiffy, mark 4. *Educational and Psychological Measurement*, **34**, 111–117.

King, J., Banerjee, S.K., Marvin, J. & Özdemir, Ö. 1982. A comparison of different magnetic methods for determining the relative grain size of magnetite in natural materials: some results from lake sediments. *Earth and Planetary Science Letters*, **59**, 404–419.

King, J.C., Turner, J., Marshall, G.J., Connolley, W.M. & Lachlan-Cope, T.A. 2004. Antarctic Peninsula climate variability and its causes as revealed by analysis of instrumental records. *Antarctic Research Series*, **79**, 17–30.

Lascu, I. & Plank, C. 2013. A new dimension to sediment magnetism: charting the spatial variability of magnetic properties across lake basins. *Global and Planetary Change*, **110**, 340–349.

Lascu, I., McLauchlan, K., Myrbo, A., Leavitt, P.R. & Banerjee, S. K. 2012. Sediment-magnetic evidence for last millennium drought conditions at the prairie–forest ecotone of northern United States. *Palaeogeography Palaeoclimatology Palaeoecology*, **337**, 99–107.

Lecomte, K.L., Vignoni, P., Córdoba, F.E., Chaparro, M.A.E., Chaparro, M.A.E., Kopalova, K., Gargiulo, J.D., Lirio, J.M., Irurzun, M.A. & Böhnel, H.N. 2016. Hydrological systems from the Antarctic Peninsula under climate change: James Ross Archipelago as study case. *Environmental Earth Sciences*, 10.1007/s12665-016-5406-y.

Li, J.H., Pan, Y.X., Liu, Q.S., Qin, H.F., Deng, C.L., Che, R.C. & Yang, X.A. 2010. A comparative study of magnetic properties between whole cells and isolated magnetosomes of *Magnetospirillum magneticum* AMB-1. *Chinese Science Bulletin*, **55**, 38–44.

Liu, Q.S., Roberts, A.P., Larrasoaña, J.C., Banerjee, S.K., Guyodo, Y., Tauxe, L. & Oldfield, F. 2012. Environmental magnetism: principles and applications. *Review of Geophysics*, 10.1029/2012RG000393.

Ludwig, P., Egli, R., Bishop, S., Chernenko, V., Frederichs, T., Rugel, G., Merchel, S. & Orgeira, M.J. 2013. Characterization of primary and secondary magnetite in marine sediment by combining chemical and magnetic unmixing techniques. *Global and Planetary Change*, **110**, 321–339.

Maher, B.A., Thompson, R. & Hounslow, M.W. 1999. Introduction. *In* Maher, B.A. & Thompson, R., *eds. Quaternary climate, environments and magnetism*. Cambridge: Cambridge University Press, 1–48.

Namiesnik, J. & Szefer, P., *eds*. 2010. *Analytical measurements in aquatic environments*. Boca Raton, FL: CRC Press, Taylor & Francis, 506 pp.

Nedbalova, L., Nývlt, D., Kopacek, J., Sobr, M. & Elster, J. 2013. Freshwater lakes of Ulu Peninsula, James Ross Island, north-east Antarctic Peninsula: origin, geomorphology and physical and chemical limnology. *Antarctic Science*, **25**, 358–372.

Pan, Y.X., Petersen, N., Davila, A.F., Zhang, L.M., Winklhofer, M., Liu, Q.S., Hanzlik, M. & Zhu, R.X. 2005. The detection of bacterial magnetite in recent sediments of Lake Chiemsee (southern Germany). *Earth Planetary Science Letters*, **232**, 109–123.

Peters, C. & Dekkers, M.J. 2003. Selected room temperature magnetic parameters as a function of mineralogy, concentration and grain size. *Physics and Chemistry of the Earth*, **28**, 659–667.

Reinholdsson, M., Snowball, I., Zillén, L., Lenz, L., Conley, D.J. 2013. Magnetic enhancement of Baltic Sea sapropels by greigite magnetofossils. *Earth and Planetary Science Letters*, **366**, 137–150.

Roberts, A.P., Chang, L., Rowan, C.J., Horng, C.-S. & Florindo, F. 2011. Magnetic properties of sedimentary greigite (Fe_3S_4): an update. *Reviews of Geophysics*, 10.1029/2010RG000336.

Roberts, E.M., Lamanna, M.C., Clarke, J.A., Meng, J., Gorscak, E., Sertich, J.J.W., O'Connor, P.M., Claeson, K.M. & MacPhee, R.D.E. 2014. Stratigraphy and vertebrate paleoecology of Upper Cretaceous–lowest Paleogene strata on Vega Island, Antarctica. *Palaeogeography Palaeoclimatology Palaeoecology*, **402**, 55–72.

SNOWBALL, I.F. 1994. Bacterial magnetite and the magnetic properties of sediments in a Swedish lake. *Earth Planetary Science Letters*, **126**, 129–142.

SNOWBALL, I.F., ZILLEN, L. & SANDGREN, P. 2002. Bacterial magnetite in Swedish varved lake sediments: a potential bio-marker of environmental change. *Quaternary International*, **88**, 13–19.

STRELIN, J.A. & SONE, T. 1998. Rock glaciers on James Ross Island, Antarctica. *Proceedings of the Permafrost–Seventh International Conference*, **55**, 1027–1033.

WARRIER, A.K., MAHESH, B.S., MOHAN, R., SHANKAR, R., ASTHANA, R. & RAVINDRA, R. 2014. Glacial–interglacial climatic variations at the Schirmacher Oasis, East Antarctica: the first report from environmental magnetism. *Palaeogeography Palaeoclimatology Palaeoecology*, **412**, 249–260.

ZALE, R. & KARLEN, W. 1989. Lake sediment cores from the Antarctic Peninsula and surrounding islands. *Geografiska Annaler - Physical Geography*, **A71**, 211–220.

https://doi.org/10.1017/S0954102017000116 Published online by Cambridge University Press